

Condensational and collisional growth of cloud droplets in a turbulent environment[†]

XIANG-YU LI*

*Department of Meteorology and Bolin Centre for Climate Research, Stockholm University, Stockholm, Sweden;
 Nordita, KTH Royal Institute of Technology and Stockholm University, 10691 Stockholm, Sweden;
 Swedish e-Science Research Centre, www.e-science.se, Stockholm, Sweden;
 JILA and Laboratory for Atmospheric and Space Physics, University of Colorado, Boulder, CO 80303, USA*

AXEL BRANDENBURG

*Nordita, KTH Royal Institute of Technology and Stockholm University, 10691 Stockholm, Sweden;
 JILA and Laboratory for Atmospheric and Space Physics, University of Colorado, Boulder, CO 80303, USA;
 Department of Astronomy, Stockholm University, SE-10691 Stockholm, Sweden*

GUNILLA SVENSSON

*Department of Meteorology and Bolin Centre for Climate Research, Stockholm University, Stockholm, Sweden;
 Swedish e-Science Research Centre, www.e-science.se, Stockholm, Sweden*

NILS E. L. HAUGEN

*SINTEF Energy Research, 7465 Trondheim, Norway;
 Department of Energy and Process Engineering, NTNU, 7491 Trondheim, Norway*

BERNHARD MEHLIG

Department of Physics, Gothenburg University, 41296 Gothenburg, Sweden

IGOR ROGACHEVSKII

*Department of Mechanical Engineering, Ben-Gurion Univ. of the Negev, P. O. Box 653, Beer-Sheva 84105, Israel;
 Nordita, KTH Royal Institute of Technology and Stockholm University, 10691 Stockholm, Sweden*

ABSTRACT

We investigate the effect of turbulence on combined condensational and collisional growth of cloud droplets by means of highly resolved direct numerical simulations of turbulence and a superparticle approximation for droplet dynamics and collisions. The droplets are subject to turbulence as well as gravity, and their collision and coalescence efficiencies are taken to be unity. We solve the thermodynamic equations governing temperature, water-vapor mixing ratio, and the resulting supersaturation fields together with the Navier-Stokes equation. Our simulations show how droplet growth depends on both Reynolds number and upon the mean energy dissipation rate. We find that the droplet size distribution broadens with increasing Reynolds number and/or mean energy dissipation rate. Since turbulence in warm clouds has relatively small mean energy dissipation rates but large Reynolds numbers, turbulence affects the condensational growth directly through supersaturation fluctuations, and it influences collisional growth indirectly through condensation. Our simulations show that, in the absence of updraft cooling, supersaturation fluctuation-induced broadening of droplet size distributions enhances the collisional growth. This is contrary to classical (non-turbulent) condensational growth, which leads to a growing mean droplet size, but a narrower droplet size distribution. Our findings, instead, show that condensational growth facilitates collisional growth by broadening the size distribution in the tails. Our conclusions are consistent with results of laboratory experiments and of field observations, that supersaturation fluctuations are important for precipitation.

*Corresponding author address: Xiang-Yu Li, Department of Meteorology and Bolin Centre for Climate Research, Stockholm University, Stockholm, Sweden

E-mail: xiang.yu.li@su.se, Revision: 1.211

1. Introduction

It has been suggested that warm rain accounts for about 30% of the total amount of rain and for 70% of the total rain area in the tropics, which plays an important role in regulating the vertical water and energy transport of the tropical atmosphere (Lau and Wu 2003). Its rapid formation has puzzled the cloud microphysics community for about 70 years. The observed time scale of warm rain formation is known to be about 20 minutes (Stephens and Haynes 2007), which is much shorter than the theoretically predicted time scale of 8 hours (Saffman and Turner 1956). Condensational and collisional growth determine the formation of warm rain. In the absence of turbulence, condensational growth is effective for cloud condensation nuclei and cloud droplets smaller than $15\text{ }\mu\text{m}$ in radius. Since the growth rate is inversely proportional to the radius, condensational growth leads to a narrow width of the droplet-size distribution. The gravity-generated collisional growth in isolation becomes important only when the mean radius of droplets is larger than $\sim 40\text{ }\mu\text{m}$. Thus, there is a size gap of $15\text{ }\mu\text{m}$ – $40\text{ }\mu\text{m}$ where neither condensation nor collision drives the growth (Pruppacher and Klett 2012; Lamb and Verlinde 2011; Grabowski and Wang 2013). Therefore, the effect of turbulence on condensational and collisional growth has been proposed to overcome this size gap (Saffman and Turner 1956; Shaw 2003; Devenish et al. 2012; Grabowski and Wang 2013). In the meteorology community, the process of collision-coalescence is also referred to as collection, while in the astrophysical community, this process is referred to as coagulation (Li et al. 2018a). Since we assume unit collision and coalescence efficiency, we use the terminology collision in the present study.

Saffman and Turner (1956) showed that turbulent mixing enhances the droplet-collision rate, following an idea of Smoluchowsky (1917). They computed that this rate is proportional to the mean energy dissipation rate of the turbulent flow. The calculation assumes that the droplets are so small that inertial effects (see Gustavsson and Mehlig 2016, for a review) are negligible, about $10\text{ }\mu\text{m}$ in radius. More recently it has become clear that inertial effects can significantly increase the collision rate for larger droplets, with larger Stokes numbers (Sundaram and Collins 1997; Falkovich et al. 2002; Chun et al. 2005; Wilkinson et al. 2006; Salazar et al. 2008; Bec et al. 2010; Gustavsson and Mehlig 2011, 2014; Gustavsson et al. 2014; Meibohm et al. 2017). These predictions are in good agreement with direct numerical simulations (DNS) of droplet dynamics in turbulence (Bhatnagar et al. 2018b,a), but the effect applies only to droplets that are large enough that they can frequently detach from the flow, due to the formation of caustics

(Wilkinson and Mehlig 2005). This requires Stokes numbers of order unity.

Reuter et al. (1988); Grover and Pruppacher (1985); Pinsky and Khain (2004); Pinsky et al. (2007, 2008) also suggested that turbulence may cause a substantial enhancement of the collision rate, yet Koziol and Leighton (1996) found that turbulence only has a moderate effect on the collision rate. This may partially be due to small Stokes numbers.

Recently it has become feasible to study the condensational and collisional growth using DNS. Most DNS studies of droplet collisions in turbulence (Franklin et al. 2005; Ayala et al. 2008; Rosa et al. 2013; Chen et al. 2016; Woittiez et al. 2009) record collision frequencies but do not allow the droplets to coalesce and grow. It is then not possible to study how the droplet-size distribution develops. Nevertheless, those works revealed that turbulence enhances the collision rate, and the effect is larger for larger mean energy-dissipation rates. The value of the Reynolds number, by contrast, was found to be of secondary importance.

Franklin (2008), Xue et al. (2008), and Wang and Grabowski (2009) investigated the collision-coalescence processes by solving the Smoluchowski equation together with the Navier-Stokes equation using DNS. They found that the size distribution of cloud droplets is significantly enhanced by turbulence. Onishi and Seifert (2016) extended the collision-rate model of Wang and Grabowski (2009) and performed DNS at higher Reynolds number, where a Reynolds number dependency was obtained. Using a Lagrangian collision-detection method, Chen et al. (2018a) found that turbulence strongly affects the broadening of the size distribution. However, Li et al. (2018a) found that turbulence has a moderate effect on the collision-coalescence process and that the enhancement effect is sensitive to the initial width of droplet-size distributions. This finding turns out to be important for the present paper.

The effect of turbulence on condensational growth has been explored intensively. Since turbulence affects the temperature field and spatial distribution of the water-vapor mixing ratio, the supersaturation field determined by temperature and water mixing ratio is inevitably affected by turbulence. Srivastava (1989) criticized the use of volume-averaged supersaturation and proposed adopting the local supersaturation field to calculate the condensational growth of cloud droplets. This is a prototype of supersaturation fluctuations. To investigate how local supersaturation fluctuations affect the condensational droplet growth in the cloud core, Vaillancourt et al. (2002) solved the thermodynamical equations that govern the supersaturation using DNS, in the presence of a turbulent flow and taking into account updraft cooling, gravitational settling, droplet inertia, and latent-heat release. Vaillancourt et al. (2002) concluded that the width of the

droplet size distribution decreases as the turbulent mean energy-dissipation rate increases and attributed this to the decrease in the decorrelation time of the supersaturation fluctuation. Lanotte et al. (2009), Sardina et al. (2015), Sardina et al. (2018), and Siewert et al. (2017) performed DNS for condensational growth using a slightly simpler model that accounts for supersaturation fluctuations but not for details of the thermodynamics. They found that the size distribution broadens as the Reynolds number increases. Paoli and Shariff (2009) found that the entrainment-induced supersaturation fluctuations broaden the droplet-size distribution. Their study is based on stochastically forced temperature and vapor fields. Grabowski and Abade (2017) and Abade et al. (2018) came to a similar conclusion using a turbulent adiabatic-parcel model.

Most of the previous DNS studies only considered either condensational growth or collisional growth. The combined condensational and collisional growth has rarely been investigated. Recently, Saito and Gotoh (2018) studied the combined processes using DNS. They found that the width of the droplet-size distribution increases as the turbulence intensity increases. However, they did not discuss whether it is the Reynolds number or the mean energy dissipation rate that matters for the broadening. Chen et al. (2018b) employed the same model as Saito and Gotoh (2018) and concluded that droplet size distributions broaden with increasing mean energy-dissipation rate. However, they did not study the dependency of the droplet-size distribution upon the Reynolds number. Indeed, several works (Lanotte et al. 2009; Sardina et al. 2015; Li et al. 2018c) suggested that condensational growth is sensitive to the Reynolds number. Collisional growth, however, is mainly affected by the mean energy-dissipation rate (Li et al. 2018a).

In this paper, we investigate the effect of turbulence on the combined condensational and collisional growth of cloud droplets at high Reynolds numbers using DNS of turbulence. For the dynamics of the local temperature and the local water-vapor mixing ratio we use the same model as Vaillancourt et al. (2002), Saito and Gotoh (2018), and Chen et al. (2018b), save for updraft cooling (see below). We include also condensational droplet growth, in the standard fashion (Pruppacher and Klett 2012; Lamb and Verlinde 2011). Details of our implementation are given in Li et al. (2018c). The droplet dynamics in our simulations is coupled to the turbulence through Stokes force. The droplets are also subject to gravitational settling. DNS of the combined problem poses formidable challenges. Therefore we use a stochastic Monte-Carlo approximation, the superparticle method (Shima et al. 2009), for the collision-coalescence process. Strengths and weaknesses of the method were discussed by Li et al. (2018b). Since we focus on the impact of tur-

bulence on droplet growth we omit the effect of cooling due to a mean updraft.

We first investigate how condensational and collisional processes affect each other through thermodynamics and droplet dynamics. Second, we explore how the combined condensational and collisional droplet growth depends on the mean energy dissipation rate and upon the Reynolds number. We focus on the time evolution of the droplet-size distribution which is the key to cloud-climate feedback and precipitation (Shaw 2003). We show that collisional growth is enhanced by the appearance of a broadening tail of the droplet-size distribution through supersaturation fluctuations.

2. Numerical model

In this section we describe our model. The equations governing the Eulerian fields and condensation are the standard ones (Vaillancourt et al. 2002). Our implementation of the equations for the Eulerian fields and condensation is the same as in Li et al. (2018c). We refer to this paper for further details. For the collision dynamics we use the superparticle method, using the PENCIL CODE; see Li et al. (2017) for an earlier application to droplet growth using this code.

a. Eulerian fields and condensation

We follow the common approach (Vaillancourt et al. 2002) and use the Boussinesq approximation to describe the air flow, assuming that density variations are negligible except when multiplied by the gravitational acceleration; see for example Mehaddi et al. (2018). This requires temperature gradients to be small. We use the standard equations for fluid density $\rho(\mathbf{x}, t)$, fluid velocity $\mathbf{u}(\mathbf{x}, t)$, temperature $T(\mathbf{x}, t)$, and water-vapor mixing ratio $q_v(\mathbf{x}, t)$:

$$\frac{\partial \rho}{\partial t} + \nabla \cdot (\rho \mathbf{u}) = S_\rho, \quad (1)$$

$$\frac{D\mathbf{u}}{Dt} = \mathbf{F} - \rho^{-1} \nabla p + \rho^{-1} \nabla \cdot (2\nu \rho \mathbf{S}) + B\mathbf{e}_z + \mathbf{S}_u, \quad (2)$$

$$\frac{DT}{Dt} = \kappa \nabla^2 T + \frac{L}{c_p} C_d, \quad (3)$$

$$\frac{Dq_v}{Dt} = D \nabla^2 q_v - C_d, \quad (4)$$

where turbulence is driven by a stochastic forcing function \mathbf{F} (see Haugen et al. 2004, for details), $D/Dt = \partial/\partial t + \mathbf{u} \cdot \nabla$ denotes the advective derivative, and $S_{ij} = \frac{1}{2}(\partial_j u_i + \partial_i u_j) - \frac{1}{3} \delta_{ij} \nabla \cdot \mathbf{u}$ is the rate-of-strain tensor (subtracting the divergence makes it traceless), p and ρ are gas pressure and density, L is the latent heat. The parameters D and κ are the diffusivities of water vapor and temperature. The source terms S_ρ and \mathbf{S}_u in Equations (1) and (2) describe mass transfer between the droplets and

the humid air due to condensation and evaporation. These terms arise because our air flow is slightly compressible (Li et al. 2018c). For an incompressible flow, these terms do not exist (Vaillancourt et al. 2002). In our case, the mass transfer is small relative to the total air mass, and the fraction of liquid to gaseous mass is also low. Therefore we neglect these terms. The pressure p and the density ρ are related to each other by an adiabatic equation of state, $p = \rho c_s^2 / \gamma$, where $\gamma = c_p / c_v = 7/5$, with $c_p = 1005 \text{ J kg}^{-1} \text{ K}^{-1}$ is the specific heat at constant pressure, and c_v is the specific heat at constant volume, respectively. For the kinematic viscosity and the thermal diffusivity of air we use $\nu = \kappa = 1.5 \times 10^{-5} \text{ m}^2 \text{ s}^{-1}$. Furthermore, $D = 2.55 \times 10^{-5} \text{ m}^2 \text{ s}^{-1}$ is the water vapor diffusivity and $L = 2.5 \times 10^6 \text{ J kg}^{-1}$ is the latent heat.

The buoyancy force $B(\mathbf{x}, t)$ is determined by temperature $T(\mathbf{x}, t)$ through $B = g(T'/T + \alpha q'_v - q_l)$, where $g = 9.81 \text{ ms}^{-2}$ is the gravitational acceleration, $T' = T - T_{\text{env}}$ is the temperature fluctuation with respect to the environmental temperature $T_{\text{env}} = 293 \text{ K}$, $\alpha = 0.608$ is the expansion coefficient, $q'_v = q_v - q_{v, \text{env}}$ is the fluctuation of the water-vapor mixing ratio (Lamb and Verlinde 2011; Kumar et al. 2014), with $q_{v, \text{env}} = 0.01 \text{ kg kg}^{-1}$; see also Li et al. (2018c). Both T and q_v are affected by droplets via the condensation rate C_d (Vaillancourt et al. 2001),

$$C_d(\mathbf{x}, t) = \frac{4\pi\rho_l G}{\rho_a} \langle s(\mathbf{x}, t) r(t) \rangle. \quad (5)$$

The average $\langle \dots \rangle$ represents a local average over droplets at position \mathbf{x} and of volume η^3 , where η is the Kolmogorov length. The parameters are: liquid-water density $\rho_l = 1000 \text{ kg m}^{-3}$, reference mass density of dry air $\rho_a = 1 \text{ kg m}^{-3}$, condensation parameter $G = 1.17 \times 10^{-10} \text{ m}^2 \text{ s}^{-1}$, supersaturation $s(\mathbf{x}, t) = q_v / q_{vs}(T) - 1$, saturated water-vapor mixing ratio $q_{vs}(T) = e_s(T) / R_v \rho_0 T$ with gas constant $R_v = 461.5 \text{ J kg}^{-1} \text{ K}^{-1}$. Finally, e_s is the saturation pressure obtained from the Clausius-Clapeyron equation (Yau and Rogers 1996; Götzfried et al. 2017), $e_s(T) = c_1 \exp(-c_2/T)$. For the two constants we choose $c_1 = 2.53 \times 10^{11} \text{ Pa}$ and $c_2 = 5420 \text{ K}$, as in Li et al. (2018c).

b. Droplet dynamics and collisions: superparticle algorithm

We approximate the droplet dynamics using the superparticle method (Zsom and Dullemond 2008; Shima et al. 2009; Johansen et al. 2012; Li et al. 2017, 2018a). In this approach, several identical microscopic droplets are represented by a superparticle. Each superparticle is assumed a certain volume and is thus assigned a droplet-number density, n_i . The position of superparticle i is denoted by \mathbf{x}_i and obeys

$$\frac{d\mathbf{x}_i}{dt} = \mathbf{V}_i, \quad (6)$$

where \mathbf{V}_i is the velocity of the superparticle. The acceleration obeys Stokes law

$$\frac{d\mathbf{V}_i}{dt} = \frac{1}{\tau_i}(\mathbf{u} - \mathbf{V}_i) + \mathbf{g}, \quad (7)$$

where τ_i is the Stokes time (Li et al. 2018a) \mathbf{u} is the fluid velocity at \mathbf{x}_i , and \mathbf{g} is the gravitational acceleration. Droplet collisions are modeled as follows (Shima et al. 2009; Johansen et al. 2012; Li et al. 2018a). When two superparticles reside in the same grid cell, the probability of collision between one droplet in a superparticle with a droplet in another superparticle during time step Δt is $p_c = \tau_c^{-1} \Delta t$. The collision time τ_c is determined by

$$\tau_c^{-1} = \sigma_c n_j |\mathbf{V}_i - \mathbf{V}_j| E_c. \quad (8)$$

Here $\sigma_c = \pi(r_i + r_j)^2$ is the cross section between two colliding droplets. The collision efficiency E_c is treated as unity. We refer to Li et al. (2017) and Li et al. (2018a) for details of the algorithm.

The superparticle method is efficient because it avoids having to follow each droplet individually. The algorithm takes into account fluctuations to a certain extent (Dziekan and Pawlowska 2017; Li et al. 2018b). This is important because our system is dilute. However, the algorithm is not microscopic, and it may exhibit certain artefacts. Nevertheless, the superparticle method has been widely used in the literature on rain formation and grain dynamics in accretion disks, because it is so efficient (Andrejczuk et al. 2008; Shima et al. 2009; Andrejczuk et al. 2010; Patterson and Wagner 2012; Riechelmann et al. 2012; Arabas and Shima 2013; Naumann and Seifert 2015, 2016; Unterstrasser et al. 2016; Dziekan and Pawlowska 2017; Li et al. 2017, 2018a; Brdar and Seifert 2018; Zsom and Dullemond 2008; Ormel et al. 2009; Zsom et al. 2010; Johansen et al. 2012; Ros and Johansen 2013; Drakowska et al. 2014; Johansen et al. 2015). The strengths and the weaknesses of the method were evaluated by Li et al. (2018b). Grabowski and Abade (2017) adapted the superparticle method to large-eddy simulations, to reach higher Reynolds numbers than possible in DNS of turbulence.

c. DNS

The present study builds upon our earlier simulations of condensational growth (Li et al. 2018c) and collisional growth (Li et al. 2018a). Here we treat both processes *together*, in order to determine how the two mechanisms interact. Our numerical setup is the same as in Li et al. (2018c), apart from the fact that we now include collisional growth. Details of our DNS solver are given in Li et al. (2017, 2018c).

To investigate how the time evolution of droplet size distribution depends on the Taylor micro-scale Reynolds

number $\text{Re}_\lambda \equiv u_{\text{rms}}^2 \sqrt{5/(3\nu\bar{\epsilon})}$ and the mean energy dissipation rate $\bar{\epsilon}$, we performed high resolution simulations with different domain sizes L_x and different non-dimensional forcing amplitude F_0 , which is a prefactor in each Fourier component of wavevector \mathbf{k} given by $F_0 c_s (|\mathbf{k}| c_s / \Delta t)^{1/2}$. We choose \mathbf{k} from a narrow band of wavevectors such that $|\mathbf{k}| L_x / 2\pi \approx 3$.

Our results are summarized in Table 1. To elucidate the combined effect of condensational and collisional growth, we use our earlier simulations as references; see Li et al. (2018c) for condensational growth and Li et al. (2018a) for collisional growth. The corresponding runs are also listed in the Table.

3. Results

a. Comparison between cases with condensational growth, collisional growth, and with both

Condensational growth of cloud droplets is affected by supersaturation fluctuations (Lanotte et al. 2009; Sardina et al. 2015; Grabowski and Abade 2017; Li et al. 2018c). These fluctuations are governed by temperature $T(\mathbf{x}, t)$ and by the water-vapor mixing ratio $q_v(\mathbf{x}, t)$. We first investigate how collision impacts these field quantities and therefore, the condensational growth. Figure 1 shows the time series of $T_{\text{rms}}(t)$, $q_{v,\text{rms}}(t)$, $B_{\text{rms}}(t)$, $s_{\text{rms}}(t)$, $q_{l,\text{rms}}(t)$, and $C_{d,\text{rms}}(t)$ with or without collisions. We see that the collisional process does not affect fluctuations of most of these quantities except for $B_{\text{rms}}(t)$ and $q_{l,\text{rms}}(t)$. The buoyancy force B is determined by temperature fluctuations T' , water-vapor mixing ratio fluctuations q'_v , and liquid-water mixing ratio q_l . The collision process leads to more intense local variations of q_l , which results in larger $q_{l,\text{rms}}$. Therefore, $B_{\text{rms}}(t)$ is enhanced by the collision process through q_l . The enhanced B , however, does not affect the flow field since the random forcing dramatically overwhelms the buoyancy force in our simulations. Thus, collisional growth does not impact the condensational growth in the present DNS.

Next, we investigate how condensational growth affects the collisional growth by comparing the time evolution of the droplet-size distribution for three different cases: condensation only, collision only, and the combined process. Figure 2(a) shows the comparison of droplet-size distributions when $\text{Re}_\lambda = 45$ and $\bar{\epsilon} = 0.039 \text{ m}^2 \cdot \text{s}^{-3}$. For the case with only condensation, the growth leads to a broadening of the size distribution. When comparing the tail of the size distribution between the cases of collision only and that of the combined process, we see that the broadening from the condensational growth facilitates the collisional growth. The combined condensational and collisional growth leads to the largest tail of the size distribution. At $t = 80 \text{ s}$, the largest radius resulting from the case of combined condensation and collision is about

$27.4 \mu\text{m}$ and the one resulting from the case of collision only is about $26.7 \mu\text{m}$. This leads to an increased rate of $27.4/26.7 - 1 \approx 3\%$. When $\text{Re}_\lambda = 130$ and $\bar{\epsilon} = 0.039 \text{ m}^2 \cdot \text{s}^{-3}$, the rate increases to $32.3/29.3 - 1 \approx 10\%$, as shown in Figure 2(b). It is worth noting that for the combined process, the droplet-size distribution exhibits an obvious transition from condensational growth to collisional growth, as shown by the dip in the droplet-size distribution. We recall that the radii of all droplets are initially $r_{\text{ini}} \equiv 10 \mu\text{m}$. After the first collision, the droplet grows to twice the mass, giving a radius of $12.6 \mu\text{m}$. Condensational growth leads to a few large droplets (close to $12.6 \mu\text{m}$ by radius) from the initially monodispersed $10 \mu\text{m}$ droplet distribution, which triggers the collision process. For the case of $\text{Re}_\lambda = 130$ (cyan curves), the dips are less abrupt. This is due to the fact that larger Re_λ leads to stronger supersaturation fluctuations, thus, generate more large droplets.

The collisional growth of cloud droplets is very sensitive to the tails of droplet-size distributions. A few large droplets can undergo a runaway collision-coalescence process by collecting small droplets. The cumulative collision time of these few large droplets is much shorter than the mean collision time (Kostinski and Shaw 2005). Thus, fluctuations play an important role in collisional growth. Condensational growth due to supersaturation fluctuations facilitates this runaway collision process by generating the few large droplets.

b. Effect of turbulence on combined condensational and collisional growth

To study the effect of turbulence on the combined condensational and collisional growth, we explore how the time evolution of droplet-size distributions depend on $\bar{\epsilon}$ and Re_λ when the growth of droplet is driven by both condensation and collision. Our previous work (Li et al. 2018c) showed that condensational growth is enhanced with increasing Re_λ but is insensitive to $\bar{\epsilon}$. Collisional growth, however, weakly depends on $\bar{\epsilon}$ and is insensitive to Re_λ (Li et al. 2018a). Therefore, we expect that the combined condensational and collisional growth depends on both Re_λ and $\bar{\epsilon}$.

Let us first inspect how the evolution of T , q_v , C_d , and s depends upon Re_λ and $\bar{\epsilon}$. Figure 3 shows that the rms values of these quantities increase as Re_λ increases, yet they depend only weakly upon $\bar{\epsilon}$. This is consistent with the result of Li et al. (2018c), which suggests that the collision process does not impact the thermodynamics. Figure 4(a) shows the time evolution of the corresponding droplet-size distributions. The first peak and its width are almost the same for different $\bar{\epsilon}$ at different times, which exhibits the same characters as the simulations without collisions in Li et al. (2018c). We attribute this feature to condensational growth and its weak dependency on $\bar{\epsilon}$. The tail of

TABLE 1. Parameter values used in the different simulation runs. Here “con” refers to condensation; “col” refers to collision; “both” refers to combined condensation and collision. Runs C1 and E1 are reference runs that agree with Runs A and C of Li et al. (2018c) (condensation only) and Runs C2 and E2 are similar to Runs A and C of Li et al. (2018a) (collisions only, except that here the initial mean number density of droplets is $n_0 = 2.5 \times 10^8 \text{ m}^{-3}$). To allow for a comparison with the reference runs, we chose the parameters for Runs A, B, C, D, and E to be the same as those by Li et al. (2018c). These authors studied *only* condensation. Here collisions and condensation are treated together.

Run	F_0	L_x (m)	N_{grid}	N_s	Processes	u_{rms} (ms^{-1})	Re_λ	$\bar{\epsilon}$ ($\text{m}^2 \text{s}^{-3}$)	$\eta \cdot 10^{-4}$ (m)	τ_η (s)	τ_L (s)
A	0.007	0.200	128^3	244140	both	0.10	44	0.005	9.2	0.056	0.67
B	0.014	0.150	128^3	244140	both	0.14	45	0.019	6.5	0.028	0.35
C	0.020	0.125	128^3	244140	both	0.16	45	0.039	5.4	0.020	0.25
C1	0.020	0.125	128^3	244140	con	0.16	45	0.039	5.4	0.020	0.25
C2	0.020	0.125	128^3	244140	col	0.16	45	0.039	5.4	0.020	0.25
D	0.020	0.250	256^3	1953120	both	0.22	78	0.039	5.4	0.020	0.37
E	0.020	0.500	512^3	15624960	both	0.28	130	0.039	5.4	0.020	0.58
E1	0.020	0.500	512^3	15624960	con	0.28	130	0.039	5.4	0.020	0.58
E2	0.020	0.500	512^3	15624960	col	0.28	130	0.039	5.4	0.020	0.58

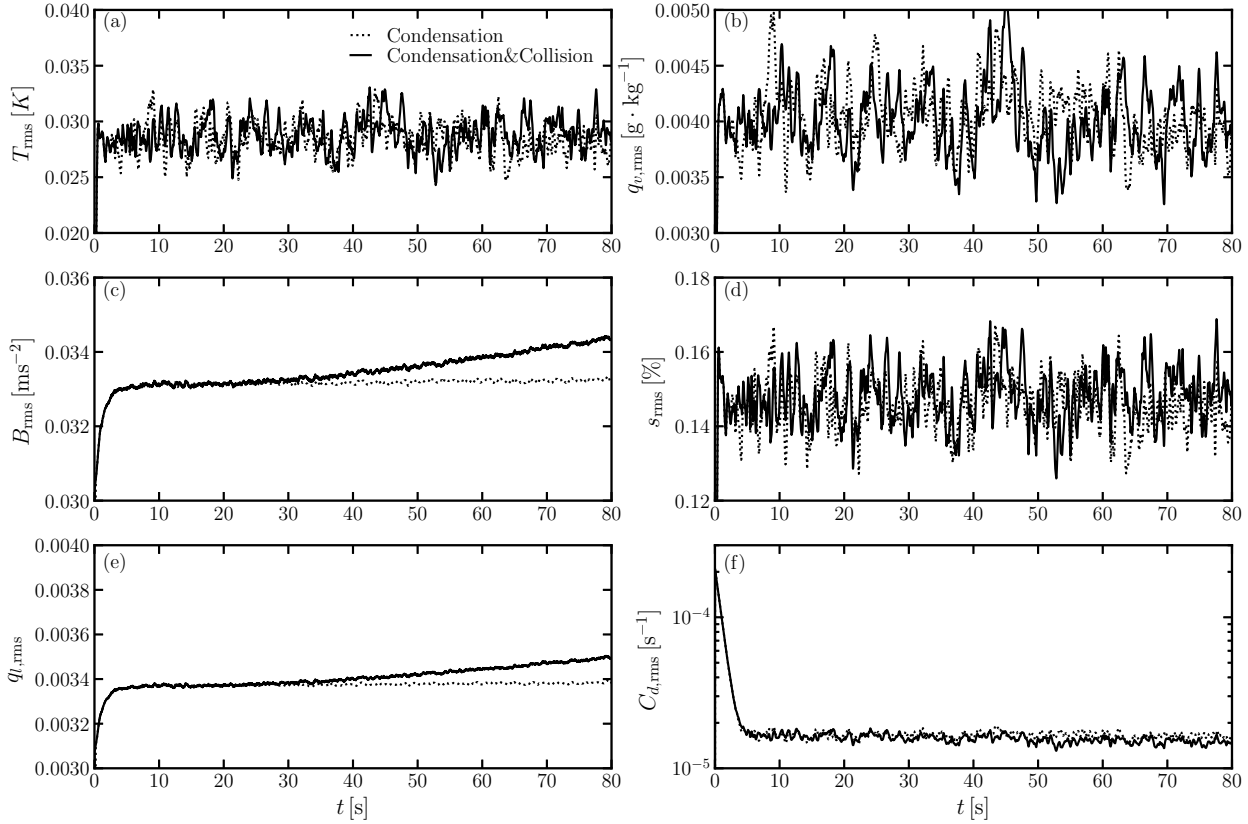


FIG. 1. Comparison of rms values of various thermodynamic quantities in the presence (absence) of collisions shown as solid (dotted) lines, corresponding to Run C (C1). Condensation is included in both cases. (a) $T_{\text{rms}}(t)$; (b) $q_{v,\text{rms}}(t)$; (c) $B_{\text{rms}}(t)$; (d) $s_{\text{rms}}(t)$; (e) $q_{l,\text{rms}}(t)$; and (f) $C_{d,\text{rms}}(t)$.

the droplet-size distribution becomes wider with increasing $\bar{\epsilon}$, which is attributed to the dependency of collisional growth on $\bar{\epsilon}$. Comparing the largest radius for the case

of $\bar{\epsilon} = 0.005 \text{ m}^2 \cdot \text{s}^{-3}$ and the case of $\bar{\epsilon} = 0.039 \text{ m}^2 \cdot \text{s}^{-3}$ at $t = 80 \text{ s}$, we find that the largest radius increases by $27/22 - 1 \approx 23\%$. Figure 4(b), on the other hand, shows

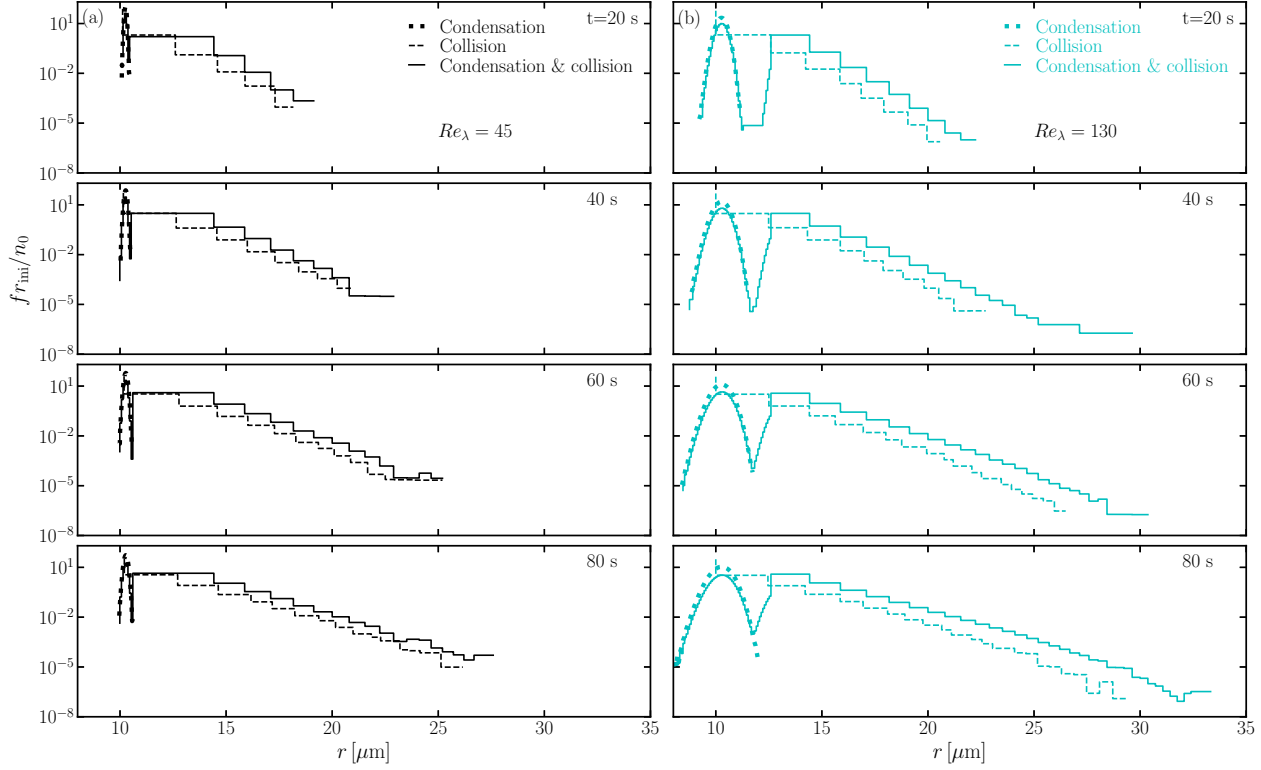


FIG. 2. Comparison of droplet-size distributions for three cases: condensational growth [Runs C1 and E1 in Table 1; Li et al. (2018c)], dotted lines; collisional growth [Runs C2 and E2 in Table 1; Li et al. (2018a)], dashed lines, and the combined processes (Runs C and E in Table 1), solid lines. (a) $Re_\lambda = 45$; (b) $Re_\lambda = 130$.

time evolution of droplet-size distributions for different Re_λ with fixed $\bar{\epsilon}$. The first peaks exhibit the same shape and dependency on Re_λ as the ones when collision was not included (Li et al. 2018c). The distributions of small droplets becomes wider with increasing Re_λ , which is due to the fact that condensational growth is enhanced with increasing Re_λ . The tail of the droplet-size distribution broadens with increasing Re_λ . This is attributed to the condensational growth and its induced collision since collisional growth only depends on $\bar{\epsilon}$. We again check the largest radius for the case of $Re_\lambda = 45$ and $Re_\lambda = 130$. The increased rate of the largest radius is $32.3/27.4 - 1 \approx 20\%$.

4. Conclusions

We investigated how the condensation and collision processes affect each other by comparing droplet-size distributions for three cases: pure condensation, pure collision, and the combined processes. We found that condensational growth broadens the droplet-size distributions in the initial phase of droplet growth, after which collisional growth is triggered. The condensation-triggered collision is pronounced with larger $Re_\lambda = 130$. The collision process only enhances the buoyancy force and does not affect

the temperature, water-vapor mixing ratio, and supersaturation. Therefore, it does not influence the condensation process.

Next, we studied the combined condensational and collisional growth at different $\bar{\epsilon}$ and Re_λ . We observed that the droplet-size distribution broadens with either increasing $\bar{\epsilon}$ or Re_λ . The dependency on Re_λ can be explained as follows. Our previous studies (Li et al. 2018a) showed that collisional growth weakly depends on $\bar{\epsilon}$ and is insensitive to Re_λ . The condensational growth, instead, strongly depends on Re_λ and is insensitive to $\bar{\epsilon}$ (Li et al. 2018c). Also, in the present study, the comparison among cases of pure condensation, pure collision, and the combined process demonstrates that condensational growth triggers the collisional growth. Therefore, we conclude that the Re_λ dependency is caused by the condensation process, which indirectly enhances the collisional growth. The combined processes are also observed to depend on $\bar{\epsilon}$, which is attributed to the dependency of the collisional growth on $\bar{\epsilon}$. However, the largest $\bar{\epsilon}$ in warm clouds is only about $\bar{\epsilon} = 10^{-3} \text{ m}^2 \text{ s}^{-3}$ (Siebert et al. 2006), so its effect on collisional growth is small (Li et al. 2018a). In reality, we have $Re_\lambda \approx 10^4$ in a cloud system. It is expected that a higher

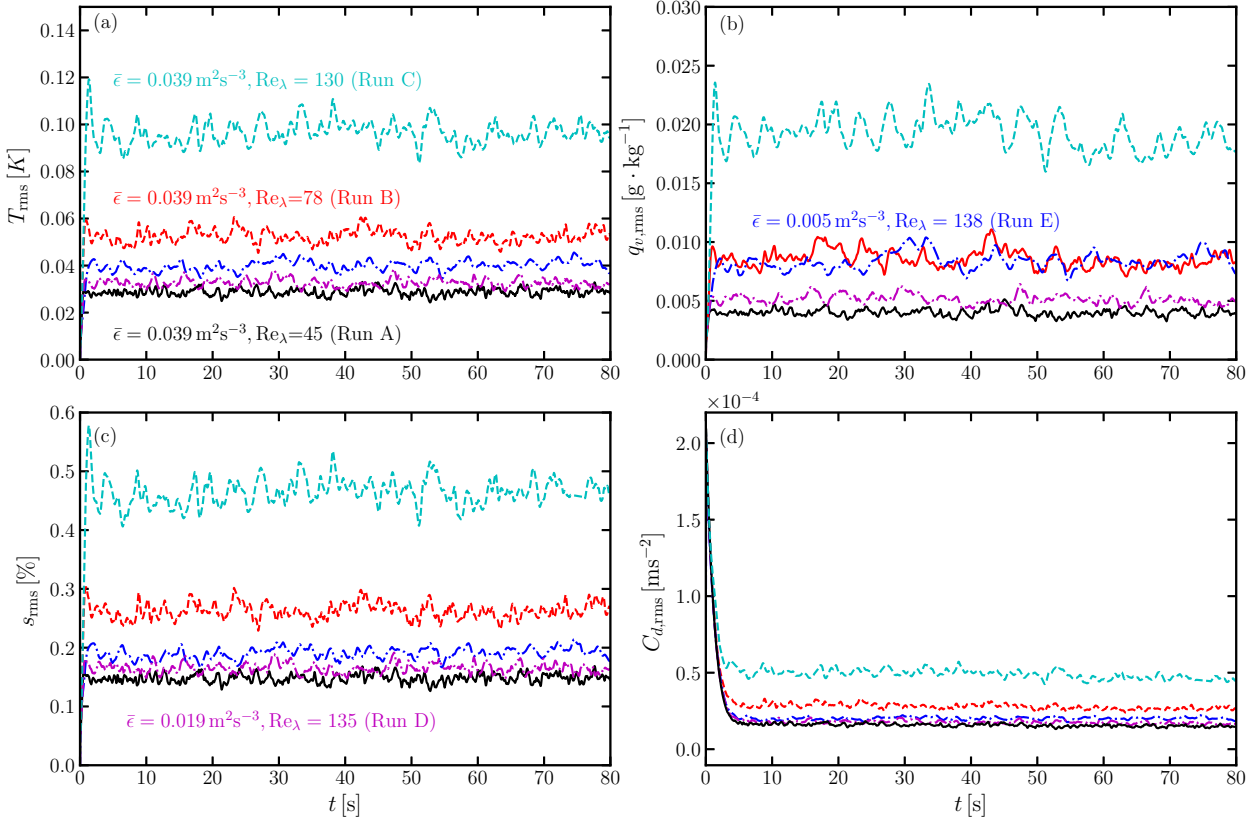


FIG. 3. Evolution of the rms values of temperature (a), water-vapor mixing ratio (b), supersaturation ratio (c), and condensation rate (d) for Runs A (black), B (red), C (cyan), D (pink), and E (blue).

Re_λ would lead to larger supersaturation fluctuations, and therefore fast broadening of the size distribution, which facilitates the collisional growth. Our findings also support results of the laboratory experiment of Chandrakar et al. (2016) that supersaturation fluctuations are likely of leading importance for precipitation formation. Furthermore, we demonstrated numerically that supersaturation fluctuations enhance the collisional growth.

In conclusion, we have found that the growth of cloud droplets in warm clouds is substantially affected by Reynolds number. The condensational growth is driven by supersaturation fluctuations. Supersaturation fluctuations are governed by fluctuations of temperature and the water-vapor mixing ratio, which were found to increase with increasing Reynolds number (Li et al. 2018c). After the droplet-size distribution has reached a certain width, collisional growth starts to dominate the growth, which is then weakly affected by the mean energy-dissipation rate. In other words, the value of the Reynolds number influences the collisional growth *indirectly* through condensation. The mean energy-dissipation rate affects both condensational and collisional growth weakly. Therefore, the combined condensational and collisional growth is in-

fluenced by both Reynolds number and the mean energy-dissipation rate.

The classical treatment of condensational growth without turbulence, and with constant supersaturation results in a larger mean radius, but a narrower width of the size distribution. This reduces the relative velocity of potentially colliding pairs as they settle through the cloud. This implies *slower* collisional growth. Contrary to the classical treatment of condensational growth, our findings demonstrate that the supersaturation fluctuation-induced condensational growth facilitates the collisional growth by broadening the width of the droplet size distribution.

Chen et al. (2018b) compared droplet size distributions for different $\bar{\epsilon}$ when both condensation and collision were included. They attributed the condensation-induced collision to the fact that “*condensational growth narrows the droplet size distribution (DSD) and provides a great number of similar-sized droplets*” (Chen et al. 2018b), which is inconsistent with our finding that condensational growth produces wider distributions with increasing Re_λ and therefore facilitates the collisional growth. However, we emphasize that there are two crucial differences compared to our present model. First, the updraft cooling included

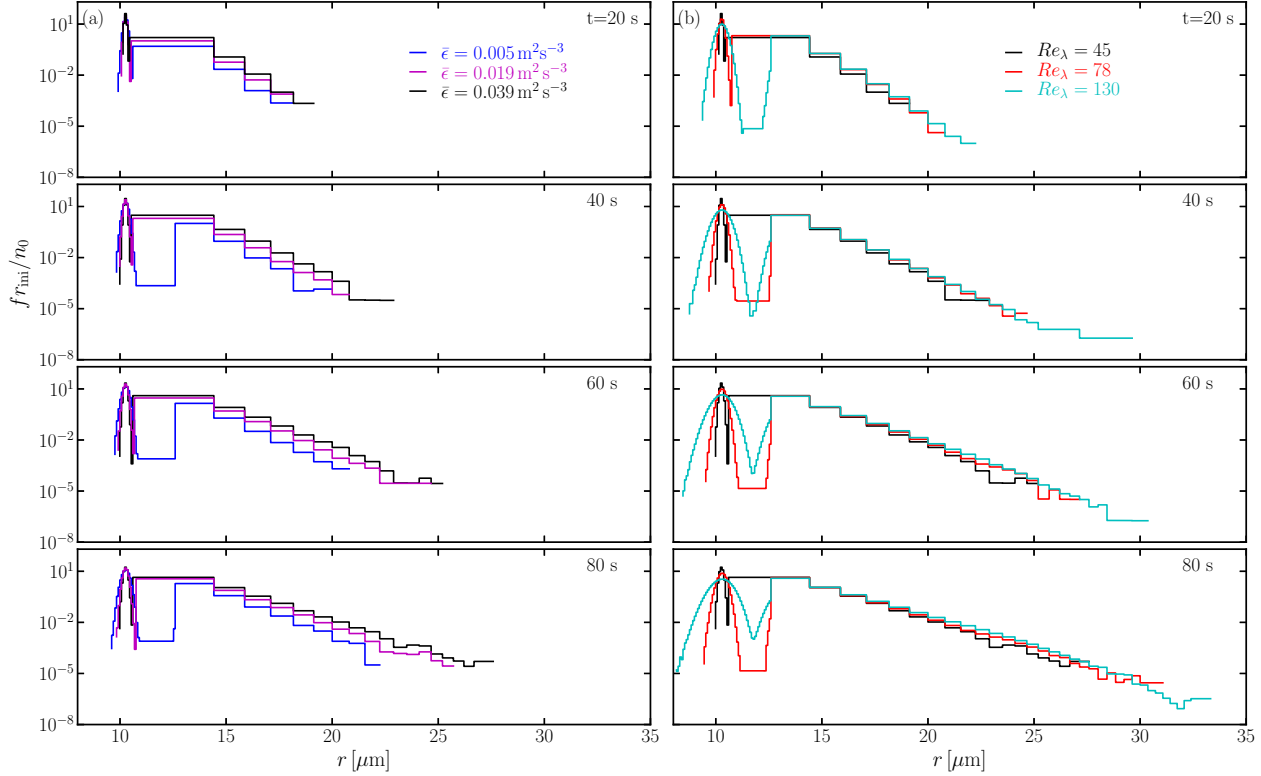


FIG. 4. Droplet size distributions for (a) different $\bar{\epsilon} = 0.005 \text{ m}^2 \text{ s}^{-3}$ (blue solid lines), 0.019 (magenta solid lines) and 0.039 (black solid line) at fixed $Re_\lambda = 45$ (see Runs A, B, and C in Table 1 for details) and for (b) different $Re_\lambda = 45$ (black solid lines), 78 (red solid lines), and 130 (cyan solid line) at fixed $\bar{\epsilon} = 0.039 \text{ m}^2 \text{ s}^{-3}$ (see Runs C, D, and E in Table 1 for details).

by Chen et al. (2018b) may suppress the supersaturation fluctuation-induced broadening of the droplet size distribution (Sardina et al. 2018). Second, they included hydrodynamic interactions between droplets. This is expected to reduce the collision and coalescence efficiency for collisions between similar-sized droplets. This may alter how turbulence affects the collisional growth by impacting the condensational growth discussed here.

As discussed at the end of Section a, our study lends some support to the notion of “lucky” droplets (Kostinski and Shaw 2005), first proposed by Telford (1955). The lucky-droplet model assumes that there is a larger droplet amongst many small ones to initiate the runaway growth (Kostinski and Shaw 2005; Wilkinson 2016). The question is where the first few lucky droplets come from. Kostinski and Shaw (2005) proposed that the first few lucky droplets could be the result of giant condensation nuclei. The present study indicates that the first few lucky droplets could result from condensational growth driven by supersaturation fluctuations caused by turbulence.

In the present study, the collision efficiency was assumed to be unity, which may substantially overesti-

mate the collisional growth. This indicates that we provide an upper boundary for the enhancement of turbulence on collisional growth. Since turbulence-induced collision efficiency is a very challenging problem (Grabowski and Wang 2013), we seek to incorporate a parameterization-free scheme of collision efficiency in the current superparticle approach. Entrainment is also omitted, which is supposed to cause strong supersaturation fluctuations. Aerosol activation is not included in the present study. Invoking all the cloud microphysical processes is computationally extremely demanding even on modern supercomputers. We strive to achieve this in future studies. Therefore, due to these limitations, we have not attempted to compare droplet-size distributions obtained from the current work with observational data.

Acknowledgements

This work was supported through the FRINATEK grant 231444 under the Research Council of Norway, SeRC, the Swedish Research Council grants 2012-5797 and 2013-03992, the University of Colorado through its support of the George Ellery Hale visiting faculty appointment, the grant “Bottlenecks for particle growth in turbulent

aerosols” from the Knut and Alice Wallenberg Foundation, Dnr. KAW 2014.0048, and Vetenskapsrådet with grant number 2017-03865. The simulations were performed using resources provided by the Swedish National Infrastructure for Computing (SNIC) at the Royal Institute of Technology in Stockholm and Chalmers Centre for Computational Science and Engineering (C3SE). This work also benefited from computer resources made available through the Norwegian NOTUR program, under award NN9405K. The source code used for the simulations of this study, the PENCIL CODE, is freely available on <https://github.com/pencil-code/>.

References

- Abade, G. C., W. W. Grabowski, and H. Pawlowska, 2018: Broadening of cloud droplet spectra through eddy hopping: Turbulent entraining parcel simulations. *Journal of the Atmospheric Sciences*, **75** (10), 3365–3379.
- Andrejczuk, M., W. W. Grabowski, J. Reisner, and A. Gadian, 2010: Cloud-aerosol interactions for boundary layer stratocumulus in the lagrangian cloud model. *Journal of Geophysical Research: Atmospheres*, **115** (D22), n/a–n/a, doi:10.1029/2010JD014248, URL <http://dx.doi.org/10.1029/2010JD014248>, d22214.
- Andrejczuk, M., J. M. Reisner, B. Henson, M. K. Dubey, and C. A. Jeffery, 2008: The potential impacts of pollution on a nondrizzling stratus deck: Does aerosol number matter more than type? *Journal of Geophysical Research: Atmospheres*, **113** (D19), n/a–n/a, doi:10.1029/2007JD009445, URL <http://dx.doi.org/10.1029/2007JD009445>, d19204.
- Arabas, S., and S.-i. Shima, 2013: Large-eddy simulations of trade wind cumuli using particle-based microphysics with monte carlo coalescence. *Journal of the Atmospheric Sciences*, **70** (9), 2768–2777, doi:10.1175/JAS-D-12-0295.1, URL <http://dx.doi.org/10.1175/JAS-D-12-0295.1>, <http://dx.doi.org/10.1175/JAS-D-12-0295.1>.
- Ayala, O., B. Rosa, and L.-P. Wang, 2008: Effects of turbulence on the geometric collision rate of sedimenting droplets. part 2. theory and parameterization. *New J. Phys.*, **10** (9), 099 802.
- Bec, J., L. Biferale, M. Cencini, A. Lanotte, and F. Toschi, 2010: Intermittency in the velocity distribution of heavy particles in turbulence. *Journal of Fluid Mechanics*, **646**, 527–536.
- Bhatnagar, A., K. Gustavsson, B. Mehlig, and D. Mitra, 2018a: Relative velocities in bi-disperse turbulent aerosols: simulations and theory. *arxiv:1809.10440*.
- Bhatnagar, A., K. Gustavsson, and D. Mitra, 2018b: Statistics of the relative velocity of particles in turbulent flows: Monodisperse particles. *Phys. Rev. E*, **97**, 023 105.
- Brdar, S., and A. Seifert, 2018: Mcsnow: A monte-carlo particle model for riming and aggregation of ice particles in a multidimensional microphysical phase space. *Journal of Advances in Modeling Earth Systems*, **10** (1), 187–206.
- Chandrakar, K. K., W. Cantrell, K. Chang, D. Ciochetto, D. Niedermeier, M. Ovchinnikov, R. A. Shaw, and F. Yang, 2016: Aerosol indirect effect from turbulence-induced broadening of cloud-droplet size distributions. *Proceedings of the National Academy of Sciences*, **113** (50), 14 243–14 248.
- Chen, S., P. Bartello, M. Yau, P. Vaillancourt, and K. Zwijssen, 2016: Cloud droplet collisions in turbulent environment: Collision statistics and parameterization. *J. Atmosph. Sci.*, **73** (2), 621–636.
- Chen, S., M. Yau, and P. Bartello, 2018a: Turbulence effects of collision efficiency and broadening of droplet size distribution in cumulus clouds. *J. Atmosph. Sci.*, **75** (1), 203–217.
- Chen, S., M.-K. Yau, P. Bartello, and L. Xue, 2018b: Bridging the condensation–collision size gap: a direct numerical simulation of continuous droplet growth in turbulent clouds. *Atmospheric Chemistry and Physics*, **18** (10), 7251–7262.
- Chun, J., D. L. Koch, S. L. Rani, A. Ahluwalia, and L. R. Collins, 2005: Clustering of aerosol particles in isotropic turbulence. *J. Fluid Mech.*, **536**, 219–251.
- Devenish, B., and Coauthors, 2012: Droplet growth in warm turbulent clouds. *Quart. J. Roy. Meteorol. Soc.*, **138** (667), 1401–1429.
- Drakowska, J., F. Windmark, and C. P. Dullemond, 2014: Modeling dust growth in protoplanetary disks: The breakthrough case. *Astron. & Astrophys.*, **567**, A38, doi:10.1051/0004-6361/201423708, 1406.0870.
- Dziekan, P., and H. Pawlowska, 2017: Stochastic coalescence in lagrangian cloud microphysics. *Atmospheric Chemistry and Physics*, **17** (22), 13 509–13 520.
- Falkovich, G., A. Fouxon, and G. Stepanov, 2002: Acceleration of rain initiation by cloud turbulence. *Nature*, **419**, 151–154.
- Franklin, C. N., 2008: A warm rain microphysics parameterization that includes the effect of turbulence. *J. Atmosph. Sci.*, **65** (6), 1795–1816.
- Franklin, C. N., P. A. Vaillancourt, M. Yau, and P. Bartello, 2005: Collision rates of cloud droplets in turbulent flow. *J. Atmosph. Sci.*, **62** (7), 2451–2466.
- Götzfried, P., B. Kumar, R. A. Shaw, and J. Schumacher, 2017: Droplet dynamics and fine-scale structure in a shearless turbulent mixing layer with phase changes. *Journal of Fluid Mechanics*, **814**, 452–483.
- Grabowski, W. W., and G. C. Abade, 2017: Broadening of cloud droplet spectra through eddy hopping: Turbulent adiabatic parcel simulations. *Journal of the Atmospheric Sciences*, **74** (5), 1485–1493.
- Grabowski, W. W., and L.-P. Wang, 2013: Growth of cloud droplets in a turbulent environment. *Annu. Rev. Fluid Mech.*, **45** (1), 293–324, <http://dx.doi.org/10.1146/annurev-fluid-011212-140750>.
- Grover, S., and H. Pruppacher, 1985: The effect of vertical turbulent fluctuations in the atmosphere on the collection of aerosol particles by cloud drops. *J. Atmosph. Sci.*, **42** (21), 2305–2318.
- Gustavsson, K., and B. Mehlig, 2011: Distribution of relative velocities in turbulent aerosols. *Physical Review E*, **84** (4), 045 304.
- Gustavsson, K., and B. Mehlig, 2014: Relative velocities of inertial particles in turbulent aerosols. *Journal of Turbulence*, **15** (1), 34–69.
- Gustavsson, K., and B. Mehlig, 2016: Statistical models for spatial patterns of heavy particles in turbulence. *Advances in Physics*, **65** (1), 1–57.
- Gustavsson, K., S. Vajedi, and B. Mehlig, 2014: Clustering of particles falling in a turbulent flow. *Phys. Rev. Lett.*, **112**, 214501.

- Haugen, N. E. L., A. Brandenburg, and W. Dobler, 2004: Simulations of nonhelical hydromagnetic turbulence. *Phys. Rev. E*, **70** (1), 016308, doi:10.1103/PhysRevE.70.016308, astro-ph/0307059.
- Johansen, A., M.-M. Mac Low, P. Lacerda, and M. Bizzarro, 2015: Growth of asteroids, planetary embryos, and kuiper belt objects by chondrule accretion. *Science Advances*, **1** (3), e1500109.
- Johansen, A., A. N. Youdin, and Y. Lithwick, 2012: Adding particle collisions to the formation of asteroids and kuiper belt objects via streaming instabilities. *Astron. Astroph.*, **537**, A125.
- Kostinski, A. B., and R. A. Shaw, 2005: Fluctuations and luck in droplet growth by coalescence. *Bull. Am. Met. Soc.*, **86**, 235–244.
- Kozioł, A. S., and H. Leighton, 1996: The effect of turbulence on the collision rates of small cloud drops. *J. Atmosph. Sci.*, **53** (13), 1910–1920.
- Kumar, B., J. Schumacher, and R. A. Shaw, 2014: Lagrangian mixing dynamics at the cloudy-clear air interface. *Journal of the Atmospheric Sciences*, **71** (7), 2564–2580, doi:10.1175/JAS-D-13-0294.1, URL <http://dx.doi.org/10.1175/JAS-D-13-0294.1>, <http://dx.doi.org/10.1175/JAS-D-13-0294.1>.
- Lamb, D., and J. Verlinde, 2011: *Physics and Chemistry of Clouds*. Cambridge, England, Cambridge Univ. Press.
- Lanotte, A. S., A. Seminara, and F. Toschi, 2009: Cloud droplet growth by condensation in homogeneous isotropic turbulence. *Journal of the Atmospheric Sciences*, **66** (6), 1685–1697, doi:10.1175/2008JAS2864.1, URL <http://dx.doi.org/10.1175/2008JAS2864.1>, <http://dx.doi.org/10.1175/2008JAS2864.1>.
- Lau, K., and H. Wu, 2003: Warm rain processes over tropical oceans and climate implications. *Geophysical Research Letters*, **30** (24).
- Li, X.-Y., A. Brandenburg, N. E. L. Haugen, and G. Svensson, 2017: Eulerian and lagrangian approaches to multidimensional condensation and collection. *Journal of Advances in Modeling Earth Systems*, **9** (2), 1116–1137.
- Li, X.-Y., A. Brandenburg, G. Svensson, N. E. L. Haugen, B. Mehlig, and I. Rogachevskii, 2018a: Effect of turbulence on collisional growth of cloud droplets. *Journal of the Atmospheric Sciences*, **75** (10), 3469–3487, doi:10.1175/JAS-D-18-0081.1, URL <https://doi.org/10.1175/JAS-D-18-0081.1>, <https://doi.org/10.1175/JAS-D-18-0081.1>.
- Li, X.-Y., B. Mehlig, G. Svensson, A. Brandenburg, and N. E. Haugen, 2018b: Fluctuations and growth histories of cloud droplets: superparticle simulations of the collision-coalescence process. *arXiv preprint arXiv:1810.07475*.
- Li, X.-Y., G. Svensson, A. Brandenburg, and N. E. Haugen, 2018c: Cloud droplets growth due to supersaturation fluctuations in stratiform clouds. *arXiv preprint arXiv:1806.10529*.
- Mehaddi, R., F. Candelier, and B. Mehlig, 2018: Inertial drag on a sphere settling in a stratified fluid. *arXiv preprint arXiv:1802.10416*.
- Meibohm, J., L. Pistone, K. Gustavsson, and B. Mehlig, 2017: Relative velocities in bidisperse turbulent suspensions. *Physical Review E*, **96** (6), 061102.
- Naumann, A. K., and A. Seifert, 2015: A lagrangian drop model to study warm rain microphysical processes in shallow cumulus. *Journal of Advances in Modeling Earth Systems*, **7** (3), 1136–1154, doi:10.1002/2015MS000456, URL <http://dx.doi.org/10.1002/2015MS000456>.
- Naumann, A. K., and A. Seifert, 2016: Recirculation and growth of raindrops in simulated shallow cumulus. *Journal of Advances in Modeling Earth Systems*, n/a–n/a, doi:10.1002/2016MS000631, URL <http://dx.doi.org/10.1002/2016MS000631>.
- Onishi, R., and A. Seifert, 2016: Reynolds-number dependence of turbulence enhancement on collision growth. *Atmosph. Chemistry and Physics*, **16** (19), 12441–12455.
- Ormel, C., D. Paszun, C. Dominik, and A. Tielens, 2009: Dust coagulation and fragmentation in molecular clouds-i. how collisions between dust aggregates alter the dust size distribution. *Astronomy & Astrophysics*, **502** (3), 845–869.
- Paoli, R., and K. Shariff, 2009: Turbulent condensation of droplets: direct simulation and a stochastic model. *Journal of the Atmospheric Sciences*, **66** (3), 723–740.
- Patterson, R. I., and W. Wagner, 2012: A stochastic weighted particle method for coagulation–advection problems. *SIAM Journal on Scientific Computing*, **34** (3), B290–B311.
- Pinsky, M., and A. Khain, 2004: Collisions of small drops in a turbulent flow. part ii: Effects of flow accelerations. *J. Atmosph. Sci.*, **61** (15), 1926–1939.
- Pinsky, M., A. Khain, and H. Krugliak, 2008: Collisions of cloud droplets in a turbulent flow. part v: Application of detailed tables of turbulent collision rate enhancement to simulation of droplet spectra evolution. *J. Atmosph. Sci.*, **65** (2), 357–374.
- Pinsky, M., A. Khain, and M. Shapiro, 2007: Collisions of cloud droplets in a turbulent flow. part iv: Droplet hydrodynamic interaction. *J. Atmosph. Sci.*, **64** (7), 2462–2482.
- Pruppacher, H. R., and J. D. Klett, 2012: *Microphysics of Clouds and Precipitation: Reprinted 1980*. Springer Science & Business Media.
- Reuter, G., R. De Villiers, and Y. Yavin, 1988: The collection kernel for two falling cloud drops subjected to random perturbations in a turbulent air flow: a stochastic model. *J. Atmosph. Sci.*, **45** (5), 765–773.
- Riechelmann, T., Y. Noh, and S. Raasch, 2012: A new method for large-eddy simulations of clouds with lagrangian droplets including the effects of turbulent collision. *New Journal of Physics*, **14** (6), 065008, URL <http://stacks.iop.org/1367-2630/14/i=6/a=065008>.
- Ros, K., and A. Johansen, 2013: Ice condensation as a planet formation mechanism. *Astronomy & Astrophysics*, **552**, A137.
- Rosa, B., H. Parishani, O. Ayala, W. W. Grabowski, and L.-P. Wang, 2013: Kinematic and dynamic collision statistics of cloud droplets from high-resolution simulations. *New J. Phys.*, **15** (4), 045032.
- Saffman, P. G., and J. S. Turner, 1956: On the collision of drops in turbulent clouds. *J. Fluid Mech.*, **1**, 16–30, doi:10.1017/S0022112056000020, URL http://journals.cambridge.org/article_S0022112056000020.
- Saito, I., and T. Gotoh, 2018: Turbulence and cloud droplets in cumulus clouds. *New Journal of Physics*, **20** (2), 023001.
- Salazar, J. P., J. De Jong, L. Cao, S. H. Woodward, H. Meng, and L. R. Collins, 2008: Experimental and numerical investigation of inertial particle clustering in isotropic turbulence. *J. Fluid Mech.*, **600**, 245–256.

- Sardina, G., F. Picano, L. Brandt, and R. Caballero, 2015: Continuous Growth of Droplet Size Variance due to Condensation in Turbulent Clouds. *Phys. Rev. Lett.*, **115** (18), 184501, doi:10.1103/PhysRevLett.115.184501, 1501.07051.
- Sardina, G., S. Poulain, L. Brandt, and R. Caballero, 2018: Broadening of cloud droplet size spectra by stochastic condensation: Effects of mean updraft velocity and ccn activation. *Journal of the Atmospheric Sciences*, **75** (2), 451–467.
- Shaw, R. A., 2003: Particle-turbulence interactions in atmospheric clouds. *Annu. Rev. Fluid Mech.*, **35** (1), 183–227.
- Shima, S., K. Kusano, A. Kawano, T. Sugiyama, and S. Kawahara, 2009: The super-droplet method for the numerical simulation of clouds and precipitation: a particle-based and probabilistic micro-physics model coupled with a non-hydrostatic model. *Quart. J. Roy. Met. Soc.*, **135**, 1307–1320, physics/0701103.
- Siebert, H., K. Lehmann, and M. Wendisch, 2006: Observations of small-scale turbulence and energy dissipation rates in the cloudy boundary layer. *Journal of the atmospheric sciences*, **63** (5), 1451–1466.
- Siewert, C., J. Bec, and G. Krstulovic, 2017: Statistical steady state in turbulent droplet condensation. *Journal of Fluid Mechanics*, **810**, 254–280.
- Smoluchowsky, M., 1917: Mathematical theory of the kinetics of the coagulation of colloidal solutions. *Z. f. phys. Ch.*, **19**, 129.
- Srivastava, R., 1989: Growth of cloud drops by condensation: A criticism of currently accepted theory and a new approach. *Journal of the atmospheric sciences*, **46** (7), 869–887.
- Stephens, G. L., and J. M. Haynes, 2007: Near global observations of the warm rain coalescence process. *Geophysical Research Letters*, **34** (20).
- Sundaram, S., and L. R. Collins, 1997: Collision statistics in an isotropic particle-laden turbulent suspension. *J. Fluid. Mech.*, **335**, 75–109.
- Telford, J. W., 1955: A new aspect of coalescence theory. *Journal of Meteorology*, **12** (5), 436–444.
- Unterstrasser, S., F. Hoffmann, and M. Lerch, 2016: Collection/aggregation algorithms in lagrangian cloud microphysical models: Rigorous evaluation in box model simulations. *Geoscientific Model Development Discussions*, **2016**, 1–49, doi:10.5194/gmd-2016-271, URL <http://www.geosci-model-dev-discuss.net/gmd-2016-271/>.
- Vaillancourt, P., M. Yau, P. Bartello, and W. W. Grabowski, 2002: Microscopic approach to cloud droplet growth by condensation. part ii: Turbulence, clustering, and condensational growth. *Journal of the atmospheric sciences*, **59** (24), 3421–3435.
- Vaillancourt, P., M. Yau, and W. W. Grabowski, 2001: Microscopic approach to cloud droplet growth by condensation. part i: Model description and results without turbulence. *Journal of the atmospheric sciences*, **58** (14), 1945–1964.
- Wang, L.-P., and W. W. Grabowski, 2009: The role of air turbulence in warm rain initiation. *Atmosph. Sci. Lett.*, **10** (1), 1–8.
- Wilkinson, M., 2016: Large deviation analysis of rapid onset of rain showers. *Phys. Rev. Lett.*, **116** (1), 018 501.
- Wilkinson, M., and B. Mehlig, 2005: Caustics in turbulent aerosols. *Europhys. Lett.*, **71**, 186–192.
- Wilkinson, M., B. Mehlig, and V. Bezuglyy, 2006: Caustic activation of rain showers. *Phys. Rev. Lett.*, **97**, 048501.
- Woittiez, E. J., H. J. Jonker, and L. M. Portela, 2009: On the combined effects of turbulence and gravity on droplet collisions in clouds: a numerical study. *Journal of the atmospheric sciences*, **66** (7), 1926–1943.
- Xue, Y., L.-P. Wang, and W. W. Grabowski, 2008: Growth of cloud droplets by turbulent collision–coalescence. *J. Atmosph. Sci.*, **65** (2), 331–356.
- Yau, M. K., and R. Rogers, 1996: *A short course in cloud physics*. Elsevier.
- Zsom, A., and C. P. Dullemond, 2008: A representative particle approach to coagulation and fragmentation of dust aggregates and fluid droplets. *Astron. Astrophys.*, **489** (2), 931–941.
- Zsom, A., C. Ormel, C. Güttler, J. Blum, and C. Dullemond, 2010: The outcome of protoplanetary dust growth: pebbles, boulders, or planetesimals?-ii. introducing the bouncing barrier. *Astronomy & Astrophysics*, **513**, A57.